Chapter 20
TOCSY in ROESY and ROESY in TOCSY

J. Schleucher[1], J. Quant[1], S. J. Glaser[1] and Christian Griesinger[2]

[1]*Department of Chemistry, Umeå University, KBC Building, S-90187 Umeå, Sweden*
[2]*Institut für Organische Chemie, Johann Wolfgang Goethe-University, Max-von-Laue-Str. 7, 60438 Frankfurt, Germany*

20.1 INTRODUCTION

Homonuclear TOCSY[1] and ROESY[2] experiments are essential tools for the identification of spin systems and for the measurement of internuclear distances, respectively. (ROESY has been reviewed by Bull;[3] see also Chapters 18 and 19.) TOCSY experiments rely on the transfer of polarization via J-coupling, ROESY experiments rely on dipolar relaxation. Cross peaks due to slow chemical exchange are present in both experiments. The success of TOCSY and ROESY depends critically on the performance of the mixing sequence used to accomplish polarization transfer via the desired interaction. It will be shown that because of the complicated mixing sequences used, cross relaxation and J transfer cannot easily be separated. In fact, longitudinal and transverse cross relaxation and J transfer are intimately connected, and it is the aim of this chapter to describe handy tools to estimate the contribution of either of these interactions for a given pulse sequence. Unwanted interactions must be suppressed, since they lead to artifacts that can hamper the interpretation of the spectra. For example, transfer via J-couplings alters the intensity of cross peaks in ROESY, and cross relaxation interferes with weak cross peaks in TOCSY. The offset dependence of TOCSY transfer and the offset dependence of the weighting of transverse and longitudinal cross-relaxation rates in CW ROESY is illustrated in Figure 20.1. Hartmann–Hahn transfer along the diagonal cannot be avoided in any ROESY experiment. Hartmann–Hahn transfer along the antidiagonal is a more serious drawback, which can be overcome in more sophisticated ROESY experiments. The offset dependence of the net cross-relaxation rate σ_{net} requires offset corrections to be applied if quantitative information is to be extracted from ROESY spectra.

Therefore, separation of coherent J transfer (TOCSY) and transfer via cross relaxation is an important goal in the development of multiple pulse sequences used in these experiments. In this chapter, we give a summary of theoretical tools used to analyze the performance of multiple pulse sequences in this respect. We discuss approaches to obtain cross-relaxation-free TOCSY spectra and suppression of coherent transfer and longitudinal cross relaxation in ROESY spectra. Relations between J transfer, cross relaxation, and chemical exchange for molecules of different sizes are collected in Table 20.1 (since cross-relaxation rates are strongly dependent on molecular weight, the possibility of separating cross relaxation from the other interactions is considered separately for small,

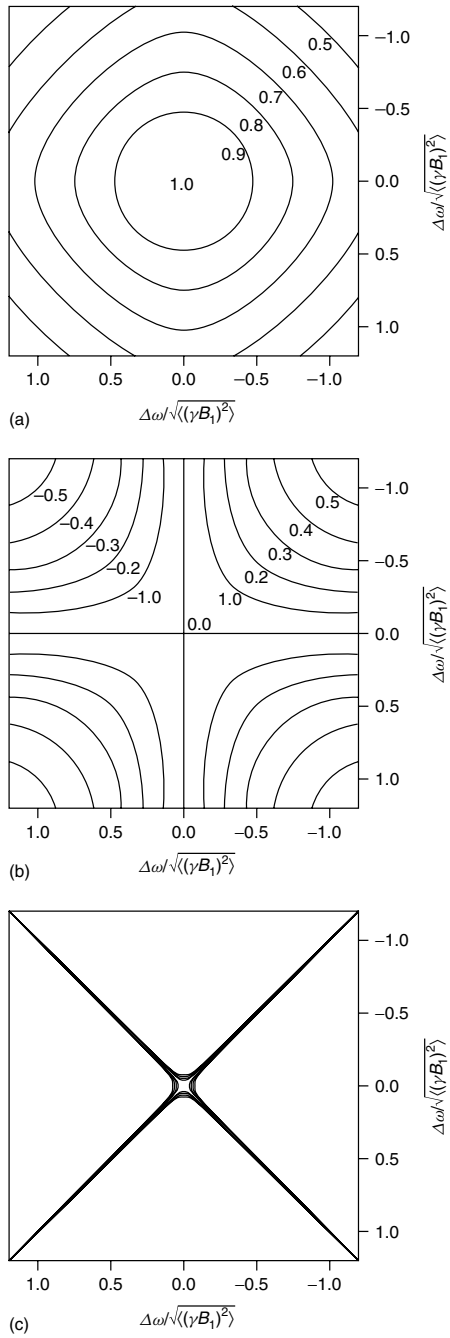

Figure 20.1. Simulation of the offset dependences of the weights of transverse (a) and longitudinal (b) cross relaxation and Hartmann–Hahn transfer (c) in CW ROESY.[11] In (c) the maximum possible Hartmann–Hahn transfer is shown as a contour plot.

medium sized, and large molecules). It is obvious from this table that for molecules of any size, longitudinal cross relaxation (NOE) can be observed without contributions from ROE or J transfer. Suppression of cross relaxation in TOCSY spectra is a problem for large molecules only. Suppression of TOCSY in ROESY spectra is necessary for molecules of any size. Chemical exchange cannot be suppressed in any experiment, but can be identified by its sign in ROESY spectra.

20.2 THEORY

20.2.1 Average Hamiltonian Theory

An arbitrary multiple pulse sequence can be represented formally by a time-dependent Hamiltonian $\hat{\mathcal{H}}(t)$. $\hat{\mathcal{H}}(t)$ can generally be represented by a series of constant Hamiltonians that act for finite intervals of time. Each Hamiltonian introduces a unitary transformation of the density matrix that is given by its propagator, and the overall effect of the multiple pulse sequence is given by the product of these propagators. Since the product of unitary transformations is again a unitary tranformation, the product of propagators can always be written as a single propagator. The Hamiltonian corresponding to this propagator is called the effective Hamiltonian $\hat{\mathcal{H}}_{\text{eff}}$ of the multiple pulse sequence. Average Hamiltonian theory[4–6] yields criteria indicating whether the effective Hamiltonian can be expressed as an 'average Hamiltonian' and whether the effective and the average Hamiltonian are the same. It also shows how the average Hamiltonian for a given $\hat{\mathcal{H}}(t)$ can be obtained. Average Hamiltonian theory is most useful if $\hat{\mathcal{H}}(t)$ fulfills two conditions:

1. $\hat{\mathcal{H}}(t)$ is periodic with a cycle time τ_{cyc}, i.e., $\hat{\mathcal{H}}(t + n\tau_{\text{cyc}}) = \hat{\mathcal{H}}(t)$;
2. the state of the spin system is only sampled at times $n\tau_{\text{cyc}}$.

These conditions are generally fulfilled for multiple pulse sequences used for TOCSY and ROESY. $\hat{\mathcal{H}}(t)$ is time-dependent during each cycle of the multiple pulse sequence, and the state of the spin system is interrogated only at multiples of the cycle times, i.e., at the end of the mixing time.

To apply average Hamiltonian theory to an arbitrary multiple pulse sequence, we first note that

Table 20.1. Relations between J Transfer, Cross Relaxation, and Chemical Exchange

	TOCSY	NOESY	ROESY	EXSY
(a) Large Molecules ($\omega\tau_c >> 1$)				
J transfer		Zero for weakly coupled spins; optimally suppressed for strongly coupled spins	Suppression of J transfer and of longitudinal cross relaxation are conflicting goals	Good suppression of J transfer and both types of cross relaxation necessary and possible
Cross relaxation	Zero (clean TOCSY)	σ_{NOE}		
Exchange	Fully operative	Fully operative	Fully operative	
(b) Medium Sized Molecules ($\omega\tau_c \approx 1$)				
J transfer		Zero for weakly coupled spins; optimally suppressed for strongly coupled spins	Suppression of J transfer and maximization of transverse cross relaxation are conflicting goals	Application of NOESY yields complete suppression of cross relaxation and J transfer
Cross relaxation	Reduced transverse cross-relaxation cannot be suppressed	Not applicable, since $\sigma_{NOE} = 0$		
Exchange	Fully operative	Fully operative	Fully operative	
(c) Small Molecules ($\omega\tau_c << 1$)				
J transfer		Zero for weakly coupled spins; optimally suppressed for strongly coupled spins	Suppression of J transfer has priority since longitudinal and transverse cross relaxation have the same sign	Application of NOESY suppresses J transfer in weakly coupled spin systems; cross relaxation cannot be suppressed
Cross relaxation	Small cross-relaxation rates do not compete efficiently	σ_{NOE}		
Exchange	Fully operative	Fully operative	Fully operative	

$\hat{\mathcal{H}}(t)$ can be decomposed into a constant part $\hat{\mathcal{H}}^0$, the Hamiltonian of the spin system in the absence of any rf irradiation, and a time-dependent part $\hat{\mathcal{H}}^1(t)$, which describes the action of the multiple pulse sequence:

$$\hat{\mathcal{H}}(t) = \hat{\mathcal{H}}^0 + \hat{\mathcal{H}}^1(t),$$
$$\hat{U}(t) = T \exp\left\{ -\mathrm{i} \int_0^t [\hat{\mathcal{H}}^0 + \hat{\mathcal{H}}^1(t')]\, \mathrm{d}t' \right\} \tag{20.1}$$

The propagator $\hat{U}(t)$ has been expressed as a time integral, as a generalization of the product of two propagators. The Dyson time-ordering operator[7,8] T formally expresses the fact that in the operator product, factors with different time arguments must be arranged in order of decreasing time from left to right. The propagator $\hat{U}^1(t)$ of $\hat{\mathcal{H}}^1(t)$ takes the form

$$\hat{U}^1(t) = T \exp\left[-\mathrm{i} \int_0^t \hat{\mathcal{H}}^1(t')\, \mathrm{d}t' \right] \tag{20.2}$$

Multiple pulse sequences with the property $\hat{U}^1(t) = 1$ for multiples of the cycle time ($t = n\tau_{cyc}$) are called cyclic sequences. By definition, such sequences leave the state of the spin system unchanged after completion of a cycle. For such sequences and times $t = n\tau_{cyc}$, it is a good approach to try to split $\hat{U}(t)$ into a product of two terms:

$$\hat{U}(\tau_{cyc}) = \hat{U}^1(\tau_{cyc})\hat{\tilde{U}}(\tau_{cyc}) \tag{20.3}$$

By definition of cyclic sequences ($\hat{U}^1(\tau_{cyc}) = 1$), $\hat{\tilde{U}}(\tau_{cyc})$ alone describes the time evolution of the spin system for times $t = n\tau_{cyc}$. $\hat{\tilde{U}}(\tau_{cyc})$ is the propagator of the toggling-frame Hamiltonian $\hat{\tilde{\mathcal{H}}}^0(t)$, which is defined by transforming $\hat{\mathcal{H}}^0$ into the time-dependent coordinate system defined by the action of $\hat{\mathcal{H}}^1(t)$:

$$\hat{\tilde{\mathcal{H}}}^0(t) = [\hat{U}^1(t)^{-1}]\hat{\mathcal{H}}^0\hat{U}^1(t) \tag{20.4}$$

Looking at the time evolution of a density matrix $\hat{\sigma}(t)$, we see that this definition of $\hat{\tilde{\mathcal{H}}}^0(t)$ indeed yields a simplified description.[5] $\hat{\sigma}(t)$ can be expressed as

$$\hat{\sigma}(t) = \hat{U}^1(t)\hat{\tilde{\sigma}}(t)[\hat{U}^1(t)]^{-1} \tag{20.5}$$

Differentiation yields [note equation (20.2) and $\dot{\hat{U}}^1(t) = -\mathrm{i}\hat{\mathcal{H}}^1(t)\hat{U}^1(t)$]:

$$\begin{aligned}
&= \dot{\hat{U}}^1(t)\hat{\tilde{\sigma}}(t)[\hat{U}^1(t)]^{-1} + \hat{U}^1(t)\dot{\hat{\tilde{\sigma}}}(t)[\hat{U}^1(t)]^{-1} \\
&\quad + \hat{U}^1(t)\hat{\tilde{\sigma}}(t)\{[\hat{U}^1(t)]^{-1}\}^{\cdot} \\
&= -\mathrm{i}\hat{\mathcal{H}}^1(t)\hat{U}^1(t)\hat{\tilde{\sigma}}(t)[\hat{U}^1(t)]^{-1} \\
&\quad + \hat{U}^1(t)\dot{\hat{\tilde{\sigma}}}(t)[\hat{U}^1(t)]^{-1} \\
&\quad + \mathrm{i}\hat{U}^1(t)\hat{\tilde{\sigma}}(t)[\hat{U}^1(t)]^{-1}\hat{\mathcal{H}}^1(t) \\
&= -\mathrm{i}[\hat{\mathcal{H}}^1(t), \hat{U}^1(t)\hat{\tilde{\sigma}}(t)[\hat{U}(t)]^{-1}] \\
&\quad + \hat{U}^1(t)\dot{\hat{\tilde{\sigma}}}(t)[\hat{U}^1(t)]^{-1}
\end{aligned} \tag{20.6}$$

Inserting the definition of $\hat{\mathcal{H}}(t)$ [equation (20.1)] and equation (20.5) into the Liouville–von Neumann equation, we obtain for $\dot{\hat{\sigma}}(t)$

$$\dot{\hat{\sigma}} = -\mathrm{i}[\hat{\mathcal{H}}^0 + \hat{\mathcal{H}}^1(t), \hat{U}^1(t)\hat{\tilde{\sigma}}(t)[\hat{U}^1(t)]^{-1}] \tag{20.7}$$

Equating equation (20.6) and equation (20.7), the commutators involving $\hat{\mathcal{H}}^1(t)$ cancel, and we obtain,

$$\hat{U}^1(t)\dot{\hat{\tilde{\sigma}}}(t)[\hat{U}^1(t)]^{-1} = -\mathrm{i}[\hat{\mathcal{H}}^0, \hat{U}^1(t)\hat{\tilde{\sigma}}(t)[\hat{U}^1(t)]^{-1}] \tag{20.8}$$

Multiplying this equation by $[(\hat{U}^1(t)]^{-1}$ from the left and by $\hat{U}^1(t)$ from the right yields

$$\begin{aligned}
\dot{\hat{\tilde{\sigma}}}(t) &= -\mathrm{i}\{[\hat{U}^1(t)]^{-1}\hat{\mathcal{H}}^0\hat{U}^1(t)\hat{\tilde{\sigma}}(t) \\
&\qquad -\hat{\tilde{\sigma}}(t)[\hat{U}^1(t)]^{-1}\hat{\mathcal{H}}^0\hat{U}^1(t)\} \\
&= -\mathrm{i}[[\hat{U}^1(t)]^{-1}\hat{\mathcal{H}}^0\hat{U}^1(t), \hat{\tilde{\sigma}}(t)] \\
&= -\mathrm{i}[\hat{\tilde{\mathcal{H}}}^0(t), \hat{\tilde{\sigma}}(t)]
\end{aligned} \tag{20.9}$$

The formal solution of this equation is [note that $\sigma(0) = \hat{\tilde{\sigma}}(0)$]

$$\hat{\tilde{\sigma}}(t) = \hat{\tilde{U}}(t)\hat{\tilde{\sigma}}(0)[\hat{\tilde{U}}(t)]^{-1} = \hat{\tilde{U}}(t)\hat{\sigma}(0)[\hat{\tilde{U}}(t)]^{-1} \tag{20.10}$$

where

$$\hat{\tilde{U}}(t) = T\exp\left[-\mathrm{i}\int_0^t \hat{\tilde{\mathcal{H}}}^0(t')\,\mathrm{d}t'\right] = \exp(-\mathrm{i}\hat{\mathcal{H}}_{\mathrm{eff}}t) \tag{20.11}$$

Inserting equation (20.10) into equation (20.5), we see that the propagator given in equation (20.3) is a valid decomposition of $\hat{U}(t)$.

As has been mentioned, $\hat{\tilde{U}}(\tau_{\mathrm{cyc}})$ yields a complete description of the time evolution of the spin system under cyclic sequences. $\hat{\mathcal{H}}_{\mathrm{eff}}$ is the effective Hamiltonian. In general, the effective Hamiltonian has the form

$$\hat{\mathcal{H}}_{\mathrm{eff}} = \hat{\mathcal{H}}_{\mathrm{eff}}^{\mathrm{lin}} + \hat{\mathcal{H}}_{\mathrm{eff}}^{\mathrm{bil}} + \hat{O}(\geq 3) \tag{20.12}$$

The terms that are linear in spin operators are collected in $\hat{\mathcal{H}}_{\mathrm{eff}}^{\mathrm{lin}}$:

$$\hat{\mathcal{H}}_{\mathrm{eff}}^{\mathrm{lin}} = \sum_k \sum_\mu c_{k\mu}\hat{I}_{k\mu} \tag{20.13}$$

with $\mu = x$, y, or z. With the help of the coefficients $c_{k\mu}$, the effective offset of spin k may be defined as

$$\Omega_k^{\mathrm{eff}} = \sqrt{\sum_\mu |c_{k\mu}|^2} \tag{20.14}$$

Terms that are bilinear in spin operators are summarized in $\hat{\mathcal{H}}_{\mathrm{eff}}^{\mathrm{bil}}$, which may be used to define effective coupling constants J_{kl}^{eff}. All terms that contain products of three or more spin operators are represented in Equation (20.12) by $\hat{O}(\geq 3)$.

$\hat{\mathcal{H}}_{\mathrm{eff}}$ can be expanded with the help of the Magnus expansion.[5,9] The zeroth-order term in the Magnus expansion is the average Hamiltonian $\hat{\bar{\mathcal{H}}}$, which is given by

$$\hat{\bar{H}} = \frac{1}{\tau_{\mathrm{cyc}}}\int_0^{\tau_{\mathrm{cyc}}} \hat{\tilde{\mathcal{H}}}^0(t')\,\mathrm{d}t' \tag{20.15}$$

20.2.2 Hartmann–Hahn Transfer

Let us consider a system of two coupled spins $^1/_2$. The Hamiltonian for this system can be written as a sum of the Zeeman part $\hat{\mathcal{H}}_Z$ and a coupling part $\hat{\mathcal{H}}_J$:

$$\begin{aligned}
\hat{\mathcal{H}}_0 &= \hat{\mathcal{H}}_Z + \hat{\mathcal{H}}_J \\
&= \Omega_1\hat{I}_{1z} + \Omega_2\hat{I}_{2z} \\
&\quad + 2\pi J(\hat{I}_{1x}\hat{I}_{2x} + \hat{I}_{1y}\hat{I}_{2y} + \hat{I}_{1z}\hat{I}_{2z})
\end{aligned} \tag{20.16}$$

Assuming the spin system to be prepared at $t = 0$ with spin 1 polarized along z and spin 2 saturated, the initial density operator can be represented as $\hat{\rho}(0) = \hat{I}_{1z}$. For the analysis of Hartmann–Hahn

transfer, it is more convenient to decompose $\hat{\mathcal{H}}_0$ into the terms $\hat{\mathcal{H}}_0'$ and $\hat{\mathcal{H}}_0''$:

$$\hat{\mathcal{H}}_0' = (\Omega_1 - \Omega_2)\frac{\hat{I}_{1z} - \hat{I}_{2z}}{2} + 2\pi J(\hat{I}_{1x}\hat{I}_{2x} + \hat{I}_{1y}\hat{I}_{2y}) \quad (20.17a)$$

$$\hat{\mathcal{H}}_0'' = (\Omega_1 + \Omega_2)\frac{\hat{I}_{1z} + \hat{I}_{2z}}{2} + 2\pi J\hat{I}_{1z}\hat{I}_{2z} \quad (20.17b)$$

$\hat{\mathcal{H}}_0''$ does not influence the time evolution of the density operator, and can be ignored, since it commutes with both $\hat{\mathcal{H}}_0'$ and $\hat{\rho}(0) = \hat{I}_{1z}$.

The evolution of $\hat{\rho}(t)$ due to the remaining operator $\hat{\mathcal{H}}_0'$ is strongly dependent on the ratio of the coupling constant J to the difference $\Delta\Omega = (\Omega_1 - \Omega_2)$. The evolution of $\hat{\rho}(t)$ is presented in Figure 20.2 with numerical simulations for the cases $|\Delta\Omega| \gg |2\pi J_{12}|$ [(a): weak coupling limit], $|\Delta\Omega| \approx |2\pi J_{12}|$ [(b): strong coupling], and $|\Delta\Omega| \ll |2\pi J_{12}|$ [(c): Hartmann–Hahn limit].

In the weak coupling limit (Figure 20.2a), the density operator of the spin system does not evolve, so the polarization of spin 1 is invariant.

In the case of strong coupling (Figure 20.2b), the density operator evolves in an oscillatory manner. Starting from $\hat{\rho}(0) = \hat{I}_{1z}$, terms $\hat{I}_{2z}$ as well as $\hat{I}_{1y}\hat{I}_{2x} - \hat{I}_{1x}\hat{I}_{2y}$ and $\hat{I}_{1x}\hat{I}_{2x} + \hat{I}_{1y}\hat{I}_{2y}$ are created periodically. Thus, a part of the initial polarization of spin 1 ($\hat{I}_{1z}$) is periodically transferred to spin 2 ($\hat{I}_{2z}$).

In the Hartmann–Hahn limit (Figure 20.2c), only the terms $\hat{I}_{2z}$ and $\hat{I}_{1y}\hat{I}_{2x} - \hat{I}_{1x}\hat{I}_{2y}$ are formed, starting from $\hat{\rho}(0) = \hat{I}_{1z}$. The characteristic property of this limiting case is the complete transfer of polarization between the coupled spins after a time $1/(2J)$.

In the general case, the rate and maximum efficiency of transfer via scalar coupling in multiple pulse sequences is a complicated function of the exact sequence.[10,11] Such cases can be described using effective offsets $\Omega_{\text{eff},1}$ and $\Omega_{\text{eff},2}$ as well as an effective coupling constant J_{12}^{eff} (cf. equations (20.12)–(20.14)). Fulfillment of the Hartmann–Hahn

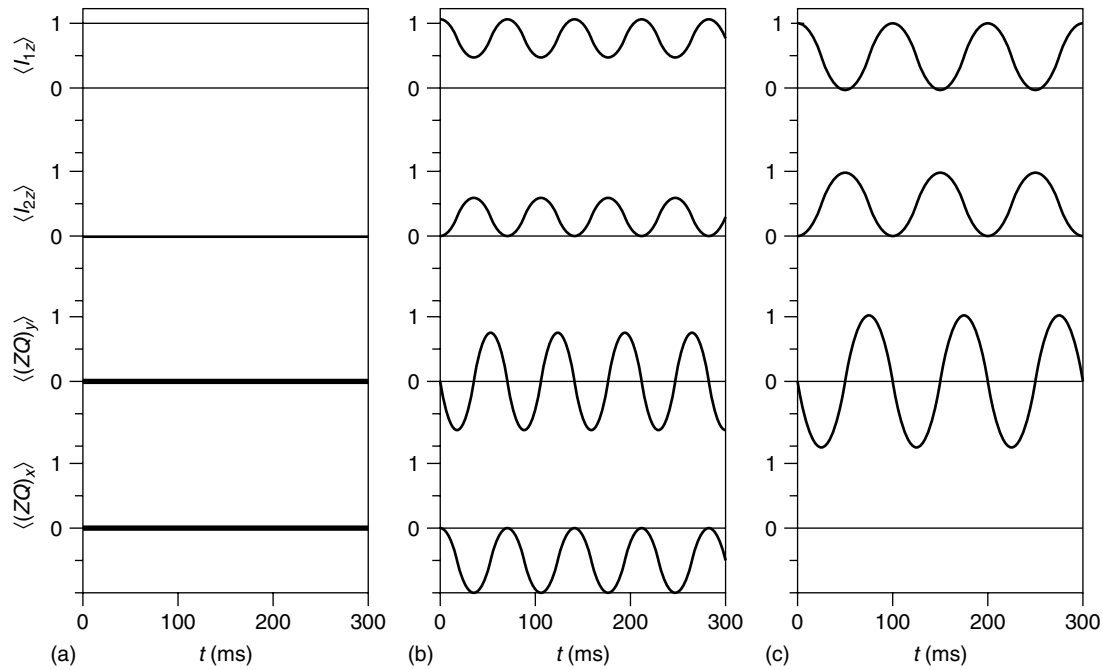

Figure 20.2. Time evolution of the initial density operator $\hat{\rho}(0) = \hat{I}_{1z}$ in a two-spin system with a coupling of 10 Hz under the influence of the Hamiltonian $\hat{\mathcal{H}}_0$. Curves from top to bottom show the expectation values of $\hat{I}_{1z}$, $\hat{I}_{2z}$, $\hat{I}_{1y}\hat{I}_{2x} - \hat{I}_{1x}\hat{I}_{2y} = (\text{ZQ})_y$ and $\hat{I}_{1x}\hat{I}_{2x} + \hat{I}_{1y}\hat{I}_{2y} = (\text{ZQ})_x$. (a) In the weak coupling limit ($|\Delta\nu| = 1000\,\text{Hz} \gg |J_{12}|$), the polarization of $\hat{I}_{1z}$ is invariant. (b) In the case of strong coupling ($|\Delta\nu| = 10\,\text{Hz} = |J_{12}|$), the polarization $\hat{I}_{1z}$ is partly transferred to $\hat{I}_{2z}$. (c) In the Hartmann–Hahn limit ($|\Delta\nu| = 0\,\text{Hz} \ll |J_{12}|$), transfer of $\hat{I}_{1z}$ to $\hat{I}_{2z}$ is complete for odd multiples of $1/2J$.

condition $|\Delta\Omega| \ll |2\pi J_{12}|$ is a necessary condition for the occurrence of Hartmann–Hahn transfer between two spins. Under the influence of a multiple pulse sequence, the Hartmann–Hahn condition takes the form $|\Delta\Omega_{\mathrm{eff}}| \ll |2\pi J_{12}^{\mathrm{eff}}|$. For spins that have similar chemical shift, corresponding to cross peaks along the diagonal of a 2D spectrum, $\Delta\Omega_{\mathrm{eff}}$ can be expressed as $\Delta\Omega_{\mathrm{eff}} = (\Delta\Omega_{\mathrm{eff}}/\Delta\Omega)\ \Delta\Omega \approx (\partial\Omega_{\mathrm{eff}}/\partial\Omega)\ \Delta\Omega = \lambda\ \Delta\Omega$. Thus, the slope λ of Ω_{eff} as a function of Ω gives a measure for the occurrence of Hartmann–Hahn transfer near the diagonal. λ is identical to the scaling factor introduced by Waugh[12] in the context of heteronuclear decoupling.

20.2.3 Invariant Trajectory Approach

Consider an uncoupled spin k subject to the action of an arbitrary multiple pulse sequence consisting of a basic sequence that is repeated during the mixing time of an experiment. The trajectory followed by a magnetization vector during the basic sequence is called invariant[13] if the orientations of the vector at the beginning and end of the basic sequence are the same. By definition, magnetization that moves on this trajectory does not experience a net rotation during a complete basic sequence. All other magnetization components experience a net rotation after each basic sequence, and are dephased by rf inhomogeneity during the repetitions of the basic sequence. The extent of dephasing depends on the effective field produced by the multiple pulse sequence, the mixing time, and the rf inhomogeneity of the probe. In this case, only the behavior of magnetization moving on the invariant trajectory need be considered in order to understand the properties of the multiple pulse sequence. The method of invariant trajectories allows an easy calculation of the effective cross relaxation rate σ_{eff} that is active during a multiple pulse sequence. For a pair of spins with identical offsets, σ_{eff} is given by

$$\sigma_{\mathrm{eff}} = w_{\mathrm{l}}\sigma_{\mathrm{NOE}} + w_{\mathrm{t}}\sigma_{\mathrm{ROE}} \tag{20.18}$$

where the weights w_{l} and w_{t} of longitudinal and transverse cross relaxation are given by the average squared longitudinal and transverse components of the invariant trajectory:[13]

$$\begin{aligned} w_{\mathrm{l}} &= \frac{1}{\tau_{\mathrm{cyc}}}\int_0^{\tau_{\mathrm{cyc}}} n_{0,z}^2(t)\,\mathrm{d}t = \langle n_{0,z}^2\rangle \\ w_{\mathrm{t}} &= \frac{1}{\tau_{\mathrm{cyc}}}\int_0^{\tau_{\mathrm{cyc}}} (n_{0,x}+n_{0,y})^2(t)\,\mathrm{d}t = \langle n_{0,(x,y)}^2\rangle \end{aligned} \tag{20.19}$$

Thus, the effective cross relaxation during a multiple pulse sequence is a linear combination of the longitudinal and transverse cross relaxation rates σ_{NOE} and σ_{ROE}, which are properties of the sample, with the weights $w_{\mathrm{l}}(\Omega)$ and $w_{\mathrm{t}}(\Omega)$, which are properties of the sequence. As an example, invariant trajectories of the phase-alternating ROESY sequence $(\pi_x\pi_{-x})_n$ for two offsets are shown in Figure 20.3. From the x, y, and z components of the invariant trajectories of this sequence (top of Figure 20.3), the weights of longitudinal and transverse cross relaxation can be obtained (bottom).

20.2.4 Connection between the Invariant Trajectory Approach and AHT

For basic sequences that create a nonzero effective field $B_{\mathrm{eff},k}$ (spin lock sequences), the orientation of the invariant trajectory is given by the orientation of $B_{\mathrm{eff},k}$.

However, there is also a more fundamental connection between invariant trajectories and effective fields. In the following discussion, we shall show that for any multiple pulse sequence, there is a relationship between the time-averaged z component of the invariant trajectory $\langle n_{0,z}\rangle$ and the slope λ of the effective field as a function of the offset.[14] This result is central to the development of ROESY sequences, since the weight of longitudinal cross relaxation is proportional to $\langle n_{0,z}^2\rangle$, while λ is a measure for the occurrence of Hartmann–Hahn transfer along the diagonal of the 2D spectrum.

In order to calculate $\lambda = \partial\Omega_{\mathrm{eff}}/\partial\Omega$ as the limit $\lim_{\Delta\Omega\to 0}\Delta\Omega_{\mathrm{eff}}/\Delta\Omega = \lim_{\Delta\Omega\to 0}(\Omega_{\mathrm{eff}} - \Omega'_{\mathrm{eff}})/\Delta\Omega$, the effective propagator $\hat{U}(\tau_{\mathrm{cyc}})$ after one cycle of duration τ_{cyc} of a repetitive multiple pulse sequence is calculated:

$$\begin{aligned} \hat{U}(\tau_{\mathrm{cyc}}) &= \prod_j \hat{U}_j = \prod_j \exp(-\mathrm{i}\hat{\mathcal{H}}_j\tau_j) \\ &= \exp(-\mathrm{i}\hat{\mathcal{H}}_{\mathrm{eff}}\tau_{\mathrm{cyc}}) \\ &= \exp[-\mathrm{i}\Omega_{\mathrm{eff}}\tau_{\mathrm{cyc}}\hat{I}_0(0)] \end{aligned} \tag{20.20}$$

$\hat{U}(\tau_{\mathrm{cyc}})$ is given by the time-ordered product of individual pulse propagators $\hat{U}_j$, which represent the propagators for individual pulses of duration τ_j and Hamiltonian $\hat{\mathcal{H}}_j$. $\hat{\mathcal{H}}_{\mathrm{eff}}$ is the effective Hamiltonian for one cycle. For a system consisting of a single spin-$^1/_2$, the effective Hamiltonian $\hat{\mathcal{H}}_{\mathrm{eff}}$ may be written as $\Omega_{\mathrm{eff}}\hat{I}_0(0)$, where Ω_{eff} is the effective chemical shift

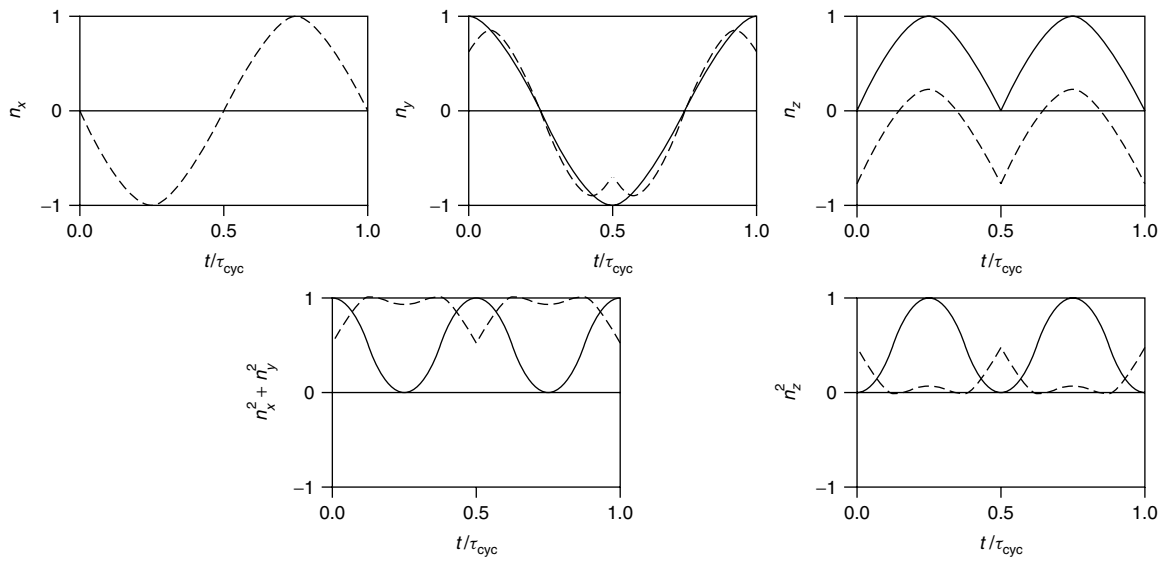

Figure 20.3. Invariant trajectories for the sequence $(\pi_x\pi_{-x})_n$ for an on-resonant spin (solid lines) and for an off-resonant spin with offset $\Omega=\gamma B_1$ (dashed lines). The x, y, and z components, together with the squares of the longitudinal and transverse components, are shown. For off-resonant spins, the sequence locks in the (y,z) plane. The weights w_t and w_l of transverse and longitudinal cross relaxation are calculated as the average square transverse and average square longitudinal components of the invariant trajectories. For the on-resonant spin, $\langle n_x^2 + n_y^2\rangle = \langle n_z^2\rangle = 0.5$, and for the off-resonant spin, $w_t = \langle n_x^2 + n_y^2\rangle = 0.88$ and $w_l = \langle n_z^2\rangle = 0.12$.

and $\hat{I}_0(0)$ defines the invariant trajectory[13] at time $t=0$:

$$\hat{\mathcal{H}}_{\text{eff}} = \Omega_{\text{eff}}\hat{I}_0(0) \tag{20.21}$$

To calculate the effective chemical shift Ω'_{eff} at the offset $\Omega' = \Omega + \Delta\Omega$, the $\hat{\mathcal{H}}_j$ are modified by $\hat{\mathcal{H}}_1 = \Delta\Omega\hat{I}_z : \hat{\mathcal{H}}'_j = \hat{\mathcal{H}}_j + \hat{\mathcal{H}}_1 = \hat{\mathcal{H}}_j + \Delta\Omega\hat{I}_z$. The resulting propagator,

$$\hat{U}'(\tau_{\text{cyc}}) = \exp(-\text{i}\hat{\mathcal{H}}'_{\text{eff}}\tau_{\text{cyc}}) = \exp[-\text{i}\Omega'_{\text{eff}}\tau_{\text{cyc}}\hat{I}'_0(0)] \tag{20.22}$$

may be divided into two factors:[4,5]

$$\hat{U}'(\tau_{\text{cyc}}) = \hat{U}(\tau_{\text{cyc}})\hat{U}_1(\tau_{\text{cyc}}) \tag{20.23}$$

with

$$\begin{aligned}\hat{U}_1(\tau_{\text{cyc}}) &= \exp(-\text{i}\hat{\mathcal{H}}_{1,\text{eff}}\tau_{\text{cyc}}) \\ &= T\exp\left\{-\text{i}\left[\int_0^{\tau_{\text{cyc}}}\hat{\tilde{\mathcal{H}}}_1(t)\,\text{d}t\right]\right\}\end{aligned} \tag{20.24}$$

where the toggling frame Hamiltonian is given by $\hat{\tilde{\mathcal{H}}}_1(t) = \hat{U}^{-1}(t)\Delta\Omega\hat{I}_z\hat{U}(t)$. In zeroth-order average Hamiltonian theory, equation (20.24) simplifies to

$$\begin{aligned}\hat{U}_1(\tau_{\text{cyc}}) &= \exp(-\text{i}\hat{\mathcal{H}}_{\text{eff},1}\tau_{\text{cyc}}) \\ &= \exp\left\{-\text{i}\left[\int_0^{\tau_{\text{cyc}}}\hat{\tilde{\mathcal{H}}}_1(t)\,\text{d}t\right]\right\}\end{aligned} \tag{20.25}$$

This simplification is justified in the limit $\Delta\Omega \to 0$. Expansion of $\hat{U}'(\tau_{\text{cyc}})$, equation (20.23), according to the Baker–Campbell–Haussdorff formula to first order yields

$$\begin{aligned}\hat{U}'(\tau_{\text{cyc}}) = \exp\{&-\text{i}(\hat{\mathcal{H}}_{\text{eff}}\tau_{\text{cyc}} + \hat{\mathcal{H}}_{\text{eff},1}\tau_{\text{cyc}}) \\ &-\tfrac{1}{2}[\hat{\mathcal{H}}_{\text{eff}}, \hat{\mathcal{H}}_{\text{eff},1}]\tau_{\text{cyc}}^2\}\end{aligned} \tag{20.26}$$

Comparing equations (20.22) and (20.26), we find

$$\begin{aligned}\hat{\mathcal{H}}'_{\text{eff}} = \Omega'_{\text{eff}}\hat{I}'_0(0) &= (\hat{\mathcal{H}}_{\text{eff}} + \hat{\mathcal{H}}_{\text{eff},1}) \\ &\quad -\tfrac{1}{2}\text{i}[\hat{\mathcal{H}}_{\text{eff}}, \hat{\mathcal{H}}_{\text{eff},1}]\tau_{\text{cyc}} \qquad (20.27\text{a}) \\ &= \Omega_{\text{eff}}\hat{I}_0(0) + \Omega_{\text{eff},1}\hat{I}_1(0) \\ &\quad -\tfrac{1}{2}\text{i}\Omega_{\text{eff}}\Omega_{\text{eff},1}[\hat{I}_0(0), \hat{I}_1(0)]\tau_{\text{cyc}} \qquad (20.27\text{b})\end{aligned}$$

where $\hat{I}_1(0)$ is defined as $\hat{\mathcal{H}}_{\text{eff},1}/\Omega_{\text{eff},1}$

For $\Delta\Omega \ll \Omega_{\text{eff}}$ and $\Delta\Omega\tau_{\text{cyc}} \ll 1$, only terms parallel to $\hat{I}_0(0)$ contribute to the magnitude of the effective field Ω'_{eff} at offset Ω'. Since the commutator $[\hat{I}_0(0),\hat{I}_1(0)]$ is perpendicular to $\hat{I}_0(0)$, the last term in equation (20.27b) may be neglected. To find the contribution of the second term of equation (20.27b), we calculate the projection of $\Omega_{\text{eff},1}\hat{I}_1(0)$ onto the direction of $\hat{I}_0(0)$. This is given by $\Omega_{\text{eff},1}\text{Tr}\{\hat{I}_0(0)\hat{I}_1(0)\}$. Thus, the magnitude of the effective field Ω'_{eff} at offset Ω' is given by

$$\Omega'_{\text{eff}} = \Omega_{\text{eff}} + \Omega_{\text{eff},1}\text{Tr}\{\hat{I}_0(0)\hat{I}_1(0)\} \quad (20.28)$$

For $\Delta\Omega \to 0$, the slope λ can be expressed as

$$\lambda = \frac{\Omega'_{\text{eff}} - \Omega_{\text{eff}}}{\Delta\Omega} = \frac{\Omega_{\text{eff},1}}{\Delta\Omega}\text{Tr}\{\hat{I}_0(0)\hat{I}_1(0)\} \quad (20.29)$$

According to equation (20.25), $\Omega_{\text{eff},1}\hat{I}_1(0) = \hat{\mathcal{H}}_{\text{eff},1}$ is given by

$$\begin{aligned}\Omega_{\text{eff},1}\hat{I}_1(0) &= \frac{1}{\tau_{\text{cyc}}}\int_0^{\tau_{\text{cyc}}} \hat{\hat{\mathcal{H}}}_1(t)\,\mathrm{d}t \\ &= \frac{1}{\tau_{\text{cyc}}}\int_0^{\tau_{\text{cyc}}} \hat{U}^{-1}(t)\Delta\Omega\hat{I}_z\hat{U}(t)\,\mathrm{d}t\end{aligned} \quad (20.30)$$

Inserting equation (20.30) into equation (20.29), we find

$$\begin{aligned}\lambda &= \frac{1}{\tau_{\text{cyc}}}\text{Tr}\left\{\hat{I}_0(0)\int_0^{\tau_{\text{cyc}}} \hat{U}^{-1}(t)\hat{I}_z\hat{U}(t)\,\mathrm{d}t\right\} \\ &= \frac{1}{\tau_{\text{cyc}}}\int_0^{\tau_{\text{cyc}}} \text{Tr}\{\hat{I}_0(0)\hat{U}^{-1}(t)\hat{I}_z\hat{U}(t)\}\,\mathrm{d}t \\ &= \frac{1}{\tau_{\text{cyc}}}\int_0^{\tau_{\text{cyc}}} \text{Tr}\{\hat{U}(t)\hat{I}_0(0)\hat{U}^{-1}(t)\hat{I}_z\}\,\mathrm{d}t \\ &= \frac{1}{\tau_{\text{cyc}}}\int_0^{\tau_{\text{cyc}}} \text{Tr}\{\hat{I}_0(t)\hat{I}_z\}\,\mathrm{d}t \\ &= \frac{1}{\tau_{\text{cyc}}}\int_0^{\tau_{\text{cyc}}} n_{0,z}(t)\,\mathrm{d}t = \langle n_{0,z}\rangle\end{aligned} \quad (20.31)$$

where $n_{0,z}(t)$ is the z component of the invariant trajectory $\hat{I}_0(t)$. The general result of equation (20.31) can be stated as follows: the slope of Ω_{eff} with respect to Ω is identical to the average z component of the invariant trajectory. Equation (20.28) relates the parameter λ central to the theory of spin decoupling to the invariant trajectory approach. We shall return to this result in 20.3.2.

20.3 SEPARATION OF HARTMANN–HAHN TRANSFER AND CROSS RELAXATION

20.3.1 Cross-Relaxation Compensated TOCSY Experiments

The TOCSY experiment is used to achieve transfer among spins in scalar-coupled spin systems. To achieve efficient TOCSY transfer, the effective fields experienced by the spins must be matched over the offset range of interest ($\lambda \ll 1$). Several multiple pulse sequences have been proposed to achieve this goal.[1,11,15–18] During these multiple pulse sequences, longitudinal and transverse cross-relaxation rates σ_{NOE} and σ_{ROE} are active and contribute to the effective cross relaxation rate σ_{eff} with the weights w_{l} and w_{t} [equation (20.18)]. Since σ_{NOE} and σ_{ROE} have the same sign for small molecules, it follows that cross-relaxation contributions cannot be suppressed near the diagonal of TOCSY spectra of small molecules, since, whatever w_{t} and w_{l} might be, the terms in equation (20.18) will always add to yield a nonvanishing σ_{eff}. Fortunately, cross-relaxation rates of such molecules are small, so that artifacts due to cross relaxation are rarely observed in the relatively short mixing times used.

As shown in Figure 20.4(a), y magnetization of on-resonant spins entering the $90^\circ_x 180^\circ_y 90^\circ_x$ composite pulse of a MLEV sequence spends equal amounts of time along longitudinal and transverse directions; therefore, $w_{\text{t}} = w_{\text{l}} = 1/2$. Since $\sigma_{\text{NOE}} = 0$ for medium sized molecules, a cross relaxation contribution $1/2\sigma_{\text{ROE}}$ results for TOCSY spectra obtained with this mixing sequence. This contribution cannot be suppressed, since this would require $w_{\text{t}} = 0$, which cannot be realized for any multiple pulse sequence. In the case of large molecules ($\sigma_{\text{ROE}}/\sigma_{\text{NOE}} = -2$), cross-relaxation rates are large, and cross relaxation can therefore compete with TOCSY transfer, leading to artifacts. It follows from equation (20.19) that for $w_{\text{t}} \approx w_{\text{l}}$, the contribution $w_{\text{t}}\sigma_{\text{ROE}}$ of transverse cross relaxation outweighs $w_{\text{l}}\sigma_{\text{NOE}}$, and a residual ROE contribution is therefore observed in TOCSY spectra of large molecules. The net cross-relaxation rate of this sequence for molecules in the spin diffusion limit is displayed in Figure 20.4(b) in units of σ_{ROE}. On resonance, ROESY cross peaks of one-quarter maximum intensity are expected to appear. From the invariant trajectory of the $90^\circ_x 180^\circ_y 90^\circ_x$ composite pulse (Figure 20.4a),

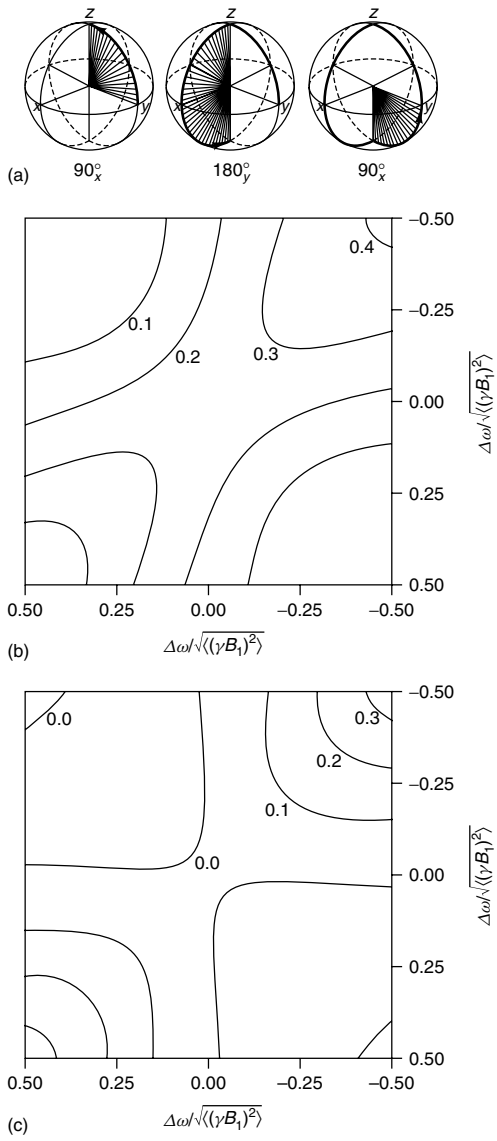

Figure 20.4. (a) Invariant trajectory starting from y magnetization for the $90^\circ_x 180^\circ_y 90^\circ_x$ composite pulse of the MLEV sequence for on-resonant irradiation. In (b) and (c), the offset dependence of the effective cross-relaxation rate σ_{eff} is shown in units of σ_{eff} in the spin diffusion limit. On-resonance, longitudinal and transverse cross relaxation have equal weights ($w_\text{l} = w_\text{t} = 1/2$). Therefore, a net cross-relaxation rate of $1/4\sigma_{\text{ROE}}$ is observed for two on-resonant spins during this sequence for a molecule in the spin diffusion limit (b). Introduction of delays of length $\Delta = \tau_{90}$ in CLEAN MLEV,[19] $90^\circ_x \Delta 180^\circ_y \Delta 90^\circ_x$, results in suppression of cross relaxation on-resonance (c).

there follows a straightforward way to eliminate this contribution for large molecules. If delays of appropriate duration ($\Delta = \tau_{90}$ for $\sigma_{\text{ROE}}/\sigma_{\text{NOE}} = -2$) are introduced into the MLEV scheme at positions where the magnetization is longitudinal, w_t and w_l can be modified such that ROE and NOE contributions cancel each other. Figure 20.4(c) shows the offset dependence of the cross-relaxation rate in the so-called CLEAN TOCSY experiment[19] obtained in this way. Cross relaxation is completely suppressed on-resonance in this experiment, while residual ROE contributions remain along the diagonal of the 2D spectrum.

While the introduction of delays is the most straightforward approach to suppress cross relaxation, and has been used frequently,[19,20] it suffers from an increase in the rf power dissipated in the sample (at constant average field strength γB_1), since the introduction of delays into any multiple pulse sequence lowers the duty ratio. This undesired effect is alleviated in more modern approaches to obtain cross relaxation compensated TOCSY mixing sequences. These approaches make use of crafted pulses to achieve a proper weighting of NOE and ROE during the multiple pulse sequence. Either the individual pulses of an existing TOCSY sequence are replaced by shaped pulses,[21] or TOCSY mixing sequences are optimized from scratch with the required weighting of NOE and ROE as a constraint,[22–24] resulting in sequences such as CITY[22] and TOWNY.[23] An example of a cross-relaxation compensated TOCSY spectrum, obtained using a MLEV mixing sequence consisting of shaped 90° pulses, is displayed in Figure 20.5.

An alternative approach to separate Hartmann–Hahn transfer and ROE was suggested by Ravikumar and Bothner-By.[25] It relies on the characteristic time evolution of coherent and incoherent magnetization transfer. However, the separation remains incomplete, since cross relaxation and coherent transfer both contain zero-frequency contributions.

20.3.2 Suppression of Hartmann–Hahn Transfer in ROESY Experiments

Using equation (20.31), which relates λ to $\langle n_{0,z} \rangle$, a relation between λ and the weight of longitudinal cross relaxation $w_\text{l} = \langle n_{0,z}^2 \rangle$ can be derived for cross peaks near the diagonal. As the inequality $\langle n_{0,z}^2 \rangle \geq \langle n_{0,z} \rangle^2$ always holds, it follows immediately that

$$w_\text{l} \geq \lambda^2 \tag{20.32}$$

This inequality shows that the suppression of longitudinal cross relaxation ($w_1 = \text{min.!}$) and of TOCSY transfer ($\lambda = \text{max.!}$) are conflicting goals. Suppression of longitudinal cross relaxation can be achieved only if TOCSY transfer is allowed, and vice versa – or, there is no ROESY without NOESY and without TOCSY. The best a sequence can do is

$$w_1 = \lambda^2 \tag{20.33}$$

This is only possible if $n_{0,z}(t)$ is constant during τ_{cyc}, as is the case in CW ROESY.[2,26,27] The latter can be described analytically in the following way. The

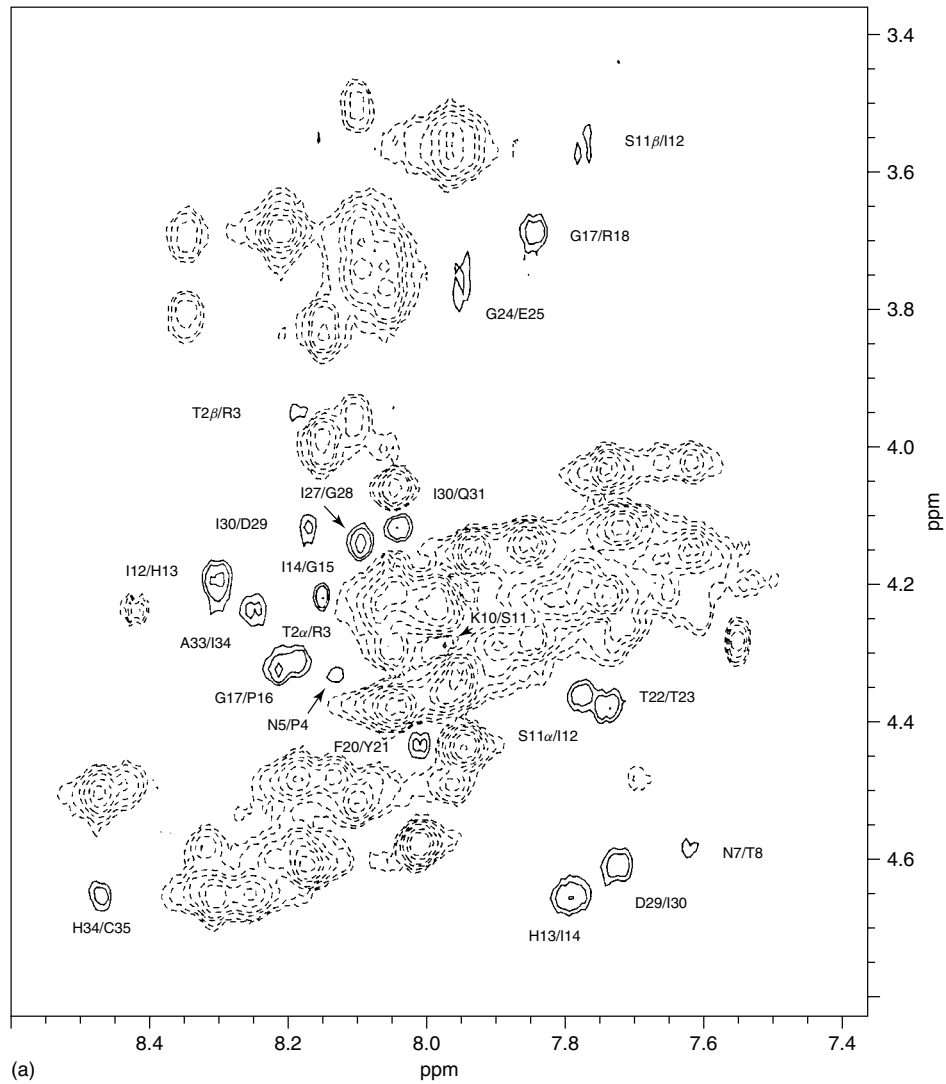

Figure 20.5. MLEV-17 spectra of the oxidized form of the peptide CTRPNNNTRKSIHIGPGRAFYTTGEIIGDIRQAHC in DMSO at 24 °C, recorded using a mean rf field strength $\gamma B_1/2\pi = 6.79$ kHz at 600 MHz. Cross peaks with the same sign as the diagonal peaks (coherent transfer) are plotted as dashed lines. Cross peaks with opposite sign (incoherent transfer) are plotted as solid lines. Only the cross-relaxation peaks are assigned. (a) In the uncompensated TOCSY experiment, strong cross peaks occur owing to cross relaxation. (b) In the TOCSY spectrum recorded using an MLEV-17 expansion of an optimized shaped 90° pulse,[21] the cross-relaxation peaks have disappeared.

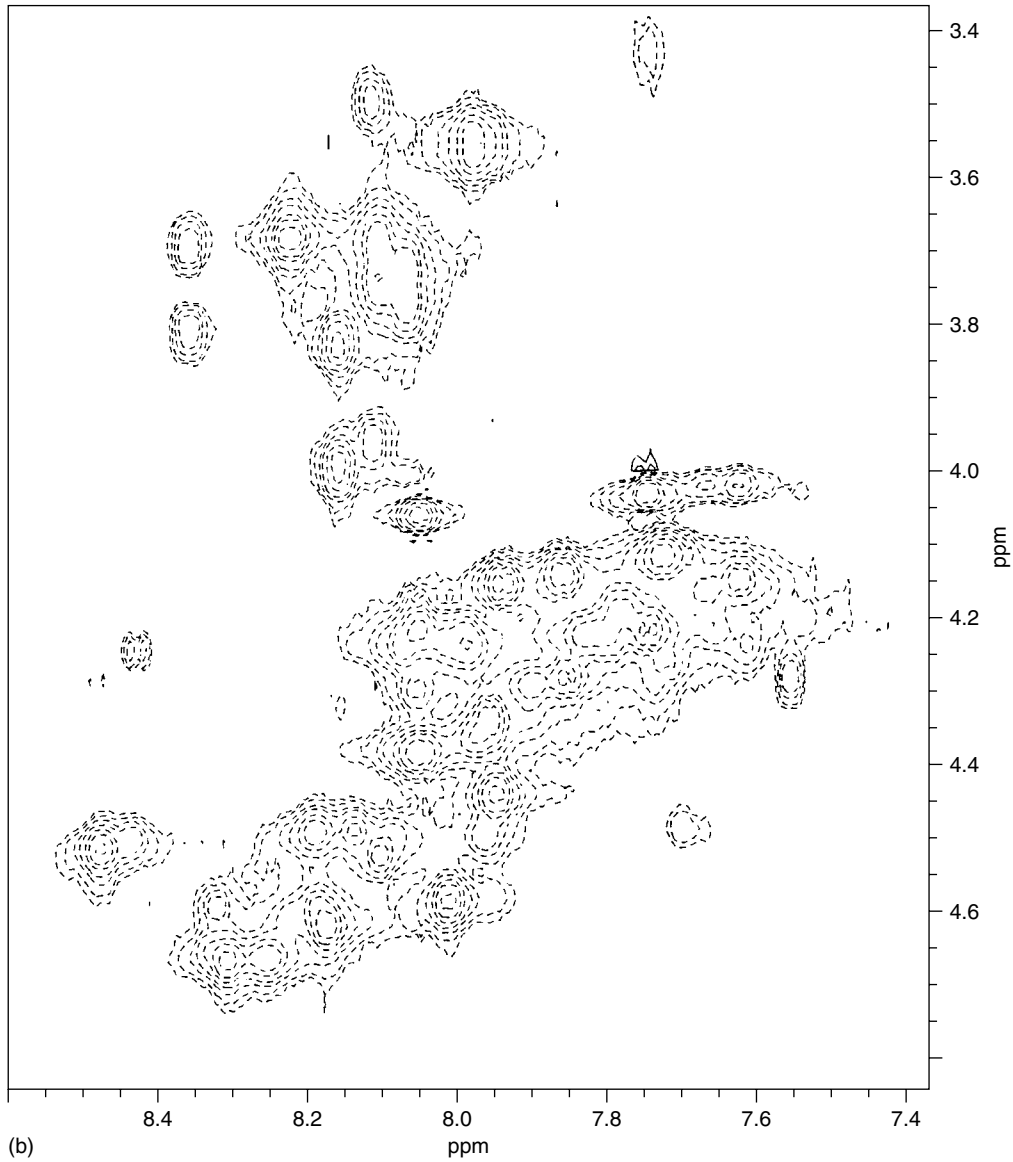

Figure 20.5. *Continued*

invariant trajectory is static and has the orientation

$$\boldsymbol{n}_0 = \cos\theta \boldsymbol{e}_z + \sin\theta \boldsymbol{e}_x, \quad \text{with } \tan\theta = \frac{\gamma B_1}{\Omega - \Omega_{\text{rf}}} \tag{20.34}$$

where γB_1 is the spin lock field strength, θ is the lock angle as measured off the z axis, and Ω_{rf} is an offset frequency of the CW irradiation. The weights for longitudinal (w_{l}) and transverse (w_{t}) cross relaxation along the diagonal are

$$w_{\text{l}} = \cos^2\theta, \quad w_{\text{t}} = \sin^2\theta \tag{20.35}$$

The effective chemical shift Ω_{eff} is given by

$$\Omega_{\text{eff}} = \sqrt{(\gamma B_1)^2 + (\Omega - \Omega_{\text{rf}})^2} \tag{20.36}$$

and the scaling $\lambda_{CW} = \partial\Omega_{eff}/\partial\Omega$ of the chemical shift of this sequence is

$$\lambda_{CW} = \frac{\partial\Omega_{eff}}{\partial\Omega} = \frac{\Omega - \Omega_{rf}}{\sqrt{(\gamma B_1)^2 + (\Omega - \Omega_{rf})^2}} = \cos\theta = \sqrt{w_l} \qquad (20.37)$$

Thus, CW ROESY has the best properties with respect to the simultaneous suppression of NOE and TOCSY that are possible, since equation (20.33) is fulfilled. For any w_t, there is no better ROESY sequence with respect to the goal of suppressing longitudinal cross relaxation and TOCSY simultaneously. In practice, a compromise must be made between the efficiency of ROESY transfer (minimization of w_l) and the degree of suppression of coherent transfer (maximization of λ). The large variation in w_l and w_t over the spectral range in CW ROESY is a strong drawback of this

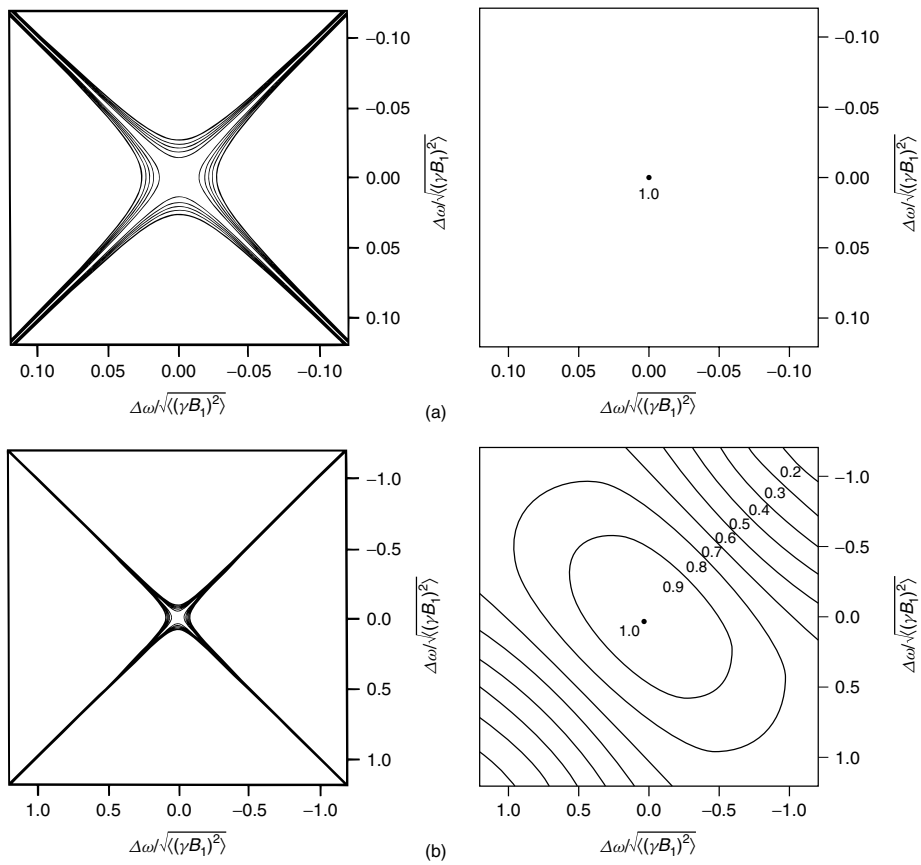

Figure 20.6. Simulations of Hartmann–Hahn transfer (left) and net cross-relaxation rate σ_{net} (right) for a molecule in the spin diffusion limit in ROESY sequences. Application of a very strong spin lock field (a) would result in a maximal σ_{net}, but complete Hartmann–Hahn matching would make such spectra useless. Reducing the spin lock field strength (b) strongly attenuates TOCSY at the expense of a relatively moderate offset dependence of σ_{net}. TOCSY transfer along the antidiagonal, as observed in (b), is suppressed by off-resonant irradiation of the spin lock field (c). However, the offset dependence of σ_{net} is much more pronounced in this case. Alternating application of two spin lock fields at opposite ends of the spectrum in JS ROESY (b) results in very smooth offset behavior, with TOCSY still being suppressed (d). Phase-alternating ROESY sequences (Figure 20.7a) show similar offset behavior for cross relaxation and coherent transfer (e). It is obvious that maximal transverse cross relaxation is achieved on-resonance at the cost of complete Hartmann–Hahn matching. Simulations of TOCSY show contour plots of the largest possible Hartmann–Hahn transfer amplitude in a two-spin system. The lowest level corresponds to a transfer amplitude of 0.1; the level spacing is 0.2.

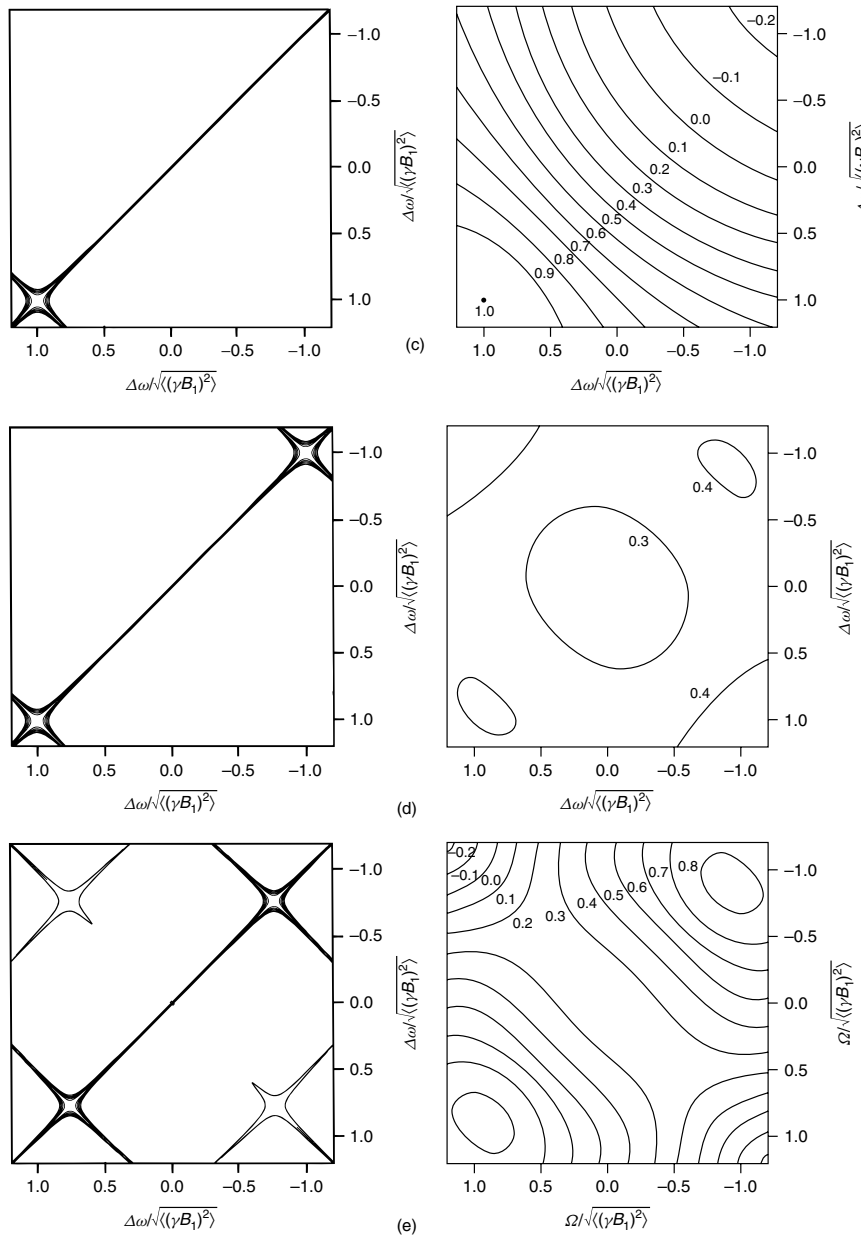

Figure 20.6. *Continued*

sequence. From an experimental point of view, an additional requirement is that w_t be uniform over the spectral width and λ not be scaled beyond a certain degree over the spectral width. A number of approaches have been proposed to address this goal.

20.3.2.1 Sequences Composed of CW Irradiations

The application of a very strong spin lock field in a ROESY experiment yields a very smooth offset dependence in CW ROESY, as displayed in

Figure 20.6(a) (left). However, the application of such strong fields is prohibitive because of serious Hartmann–Hahn transfer (Figure 20.6(a), right). Therefore, judicious choice of the spin lock field strength is important, as shown in Figure 20.6(b).[26] Furthermore, coherent transfer is much more dependent on the position of the rf irradiation frequency than cross relaxation. Therefore, coherent transfer can be reduced by judicious placement of the irradiation position (Figure 20.6c).[26,28] However, optimal placement of the transmitter offset requires prior knowledge of the coupling networks that can lead to TOCSY transfer. Without such prior knowledge, the transmitter offset has to be placed outside the spectral region according to equation (20.37) in order to avoid Hartmann–Hahn matching between any two spins. However, this results in a strong dependence of the net cross-relaxation rate on Ω, which renders the interpretation of the spectra difficult. Still, the optimal behavior of CW irradiation with respect to TOCSY suppression renders sequences employing stretches of CW irradiation attractive.

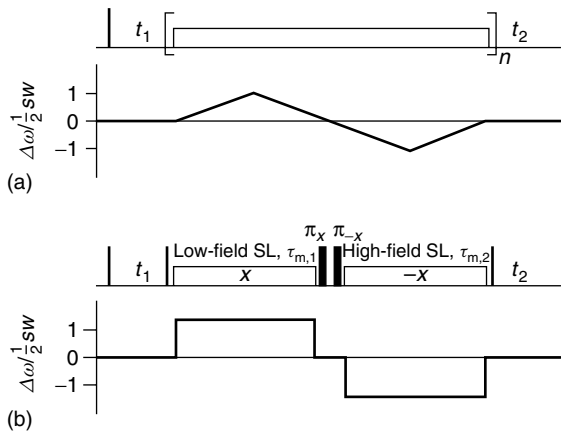

Figure 20.7. CW ROESY sequences with off-resonant irradiation spin locks. For each experiment, the pulse sequence (upper trace) and the position of the spin lock irradiation (lower trace) are given. (a) In the frequency swept variant,[29] the irradiation frequency is moved from the middle of the spectral region to the low-field edge, to the high-field edge, and back to the middle. (b) In the JS ROESY experiment, the mixing time consists of periods of low-field and high-field irradiation with a pair of 180° pulses mediating between the spin locks. The offset of the spin locks is generated by superimposing a phase gradient over a CW spin lock.

Two related approaches have been developed to deal with the stated problem. In the first, proposed by Cavanagh and Keeler,[29] the transmitter offset is swept through the offset range of the spectrum as depicted in Figure 20.7(a). This method avoids continuous irradiation at any one frequency, and therefore avoids extended periods of Hartmann–Hahn matching. However, the offset dependence of the cross-relaxation rate of this sequence has not been published, and only qualitative interpretations of such spectra appear feasible at this time. Furthermore, the programming of the frequency sweep is rather demanding from an experimental point of view.

The second approach to modify CW ROESY to obtain ROESY spectra with suppression of TOCSY transfer – the use of JS ROESY ('jump symmetrized') sequences – makes use of only two irradiation positions placed outside the low- and high-field edges of the spectrum [Figure 20.7(b)]. Since the directions of the spin lock axes differ for the high-field and the low-field spin lock for all offsets (except for $\Omega = 0$), a compensating pulse has to be applied that rotates the magnetization into the new lock direction for every offset. In the pulse sequence of JS ROESY shown in Figure 20.7(b), this is achieved by the pair of 180° pulses between the two off-resonant spin locks. The field strength of these pulses is related to the spin lock field strength and to the on-resonance lock angle θ.[14] The averaging of

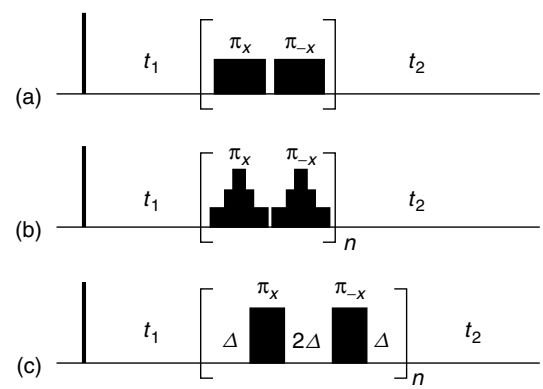

Figure 20.8. ROESY sequences employing spin locks consisting of phase-alternating pulses.[30,31]. The original sequence (a) can be modified by the use of shaped pulses (b) or by the introduction of delays (c) to increase the weight of transverse cross relaxation.

the offset dependences of the two stretches of CW irradiation results in a very smooth offset behavior and good suppression of Hartmann–Hahn transfer, as shown in Figure 20.6(d). Close to on-resonance, this sequence achieves optimal suppression of TOCSY, since λ does not differ from the optimum value [given by equation (20.37)] at any time. Further off-resonance, the performance of the sequence is reduced, since the λ value for a given offset may differ grossly for high-field and low-field CW irradiation, and must not be averaged between the extended stretches of CW irradiation. The smaller of the two λ values (of the low- and high-field irradiations) gives a measure of the occurrence of TOCSY.

20.3.2.2 $\pi_x\pi_{-x}$ *ROESY*

A second approach to obtain ROESY spectra with suppression of TOCSY transfer is the use of multiple pulse sequences optimized for this goal. Only one group of sequences has so far been proposed.[30,31] These consist of a series of phase-alternating 180° pulses $(\pi_x\pi_{-x})_n$ (Figure 20.8), where each individual 180° pulse can be rectangular (which might include delays) or shaped. Sequences using pulses with flip angles other than 180° can also be used, and have been exploited to suppress cross relaxation in exchange spectra of macromolecules.[32] For large ($\omega\tau_c \gg 1$) or intermediate sited ($\omega\tau_c \approx 1$) molecules, the unmodified mixing scheme $(\pi_x\pi_{-x})_n$ yields a net

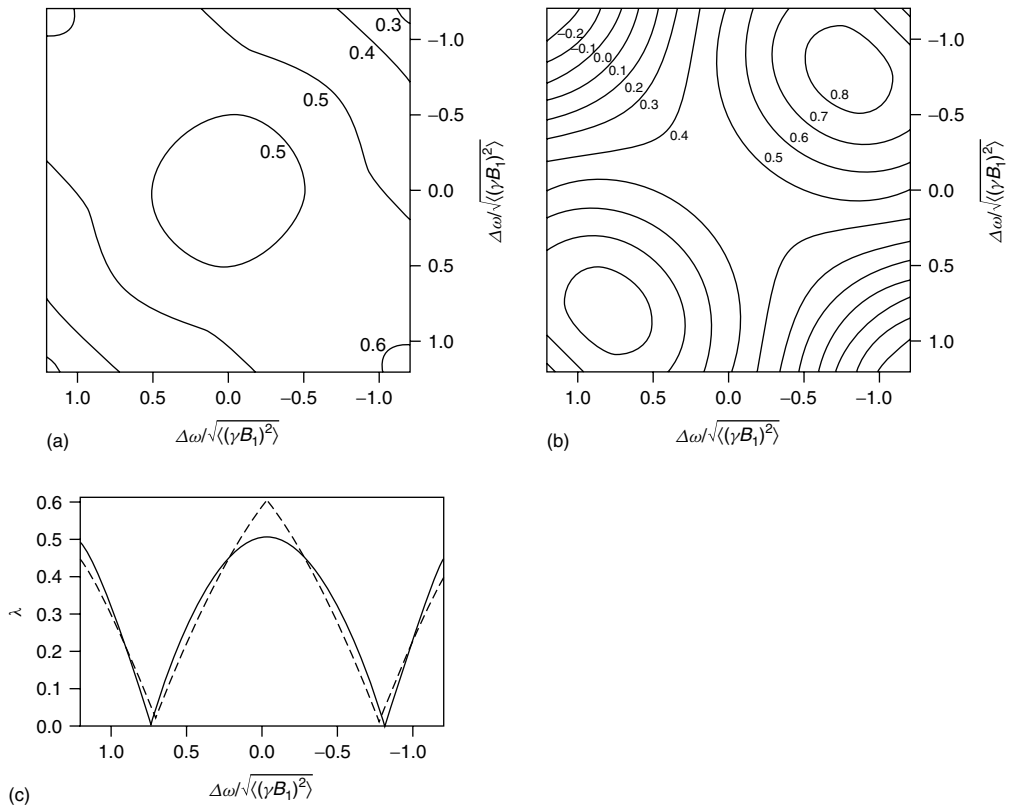

Figure 20.9. Simulations of the offset behavior of cross relaxation of JS ROESY and a ROESY employing a phase-alternating spin lock $(\pi_x^{3L}\pi_{-x}^{3L})_n$,[31] with parameters chosen to yield a net cross-relaxation rate of $0.476\sigma_{ROE}$ on-resonance. For JS ROESY (a), an on-resonance lock angle $\theta_0 = 53.77°$ was used. The phase-modulating sequence (b) yields the same net cross-relaxation rate using the shaped pulse described by Hwang *et al*.[31] The offset dependence of cross relaxation is less pronounced in JS ROESY, making direct use of intensities feasible for distance calculations. (c) Simulations of λ as a function of Ω in the offset range $\pm 1.2\sqrt{\langle(\gamma B_1)^2\rangle}$. Near on-resonance, JS ROESY suppresses TOCSY better, while the phase-alternating sequence performs better towards the edges of the spectrum.

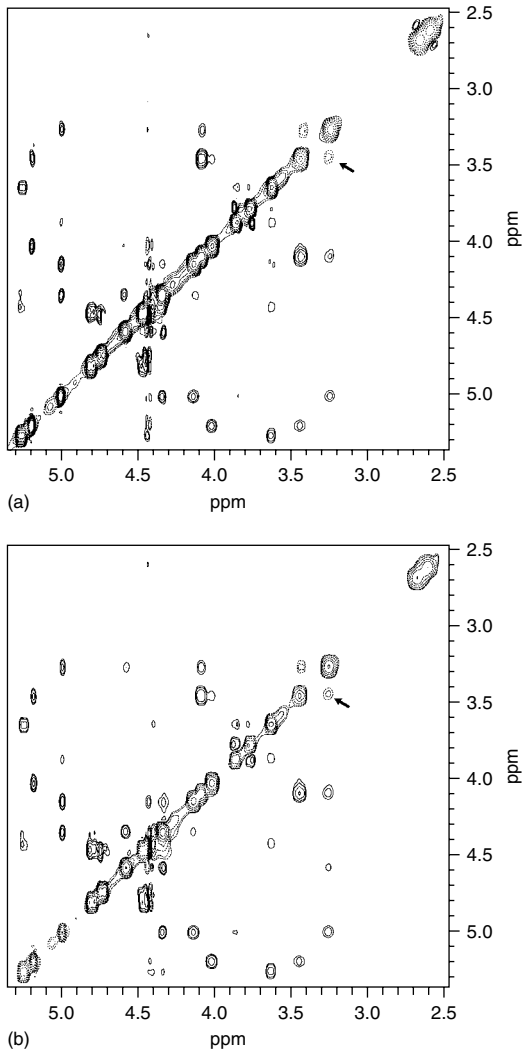

Figure 20.10. ROESY spectra of a disaccharide obtained with the ROESY sequences of (a) Figures 20.7(b) and (b) Figure 20.8(b). Positive (negative) levels are plotted as dashed (solid) lines. Both pulse sequences show similar ROE cross-peak intensities (solid contour lines). An artifact due to Hartmann–Hahn transfer between geminal protons is visible in both spectra (marked with an arrow). In contrast, no TOCSY transfer is observed between the geminal protons at 2.6 and 2.7 ppm, although they are even more strongly coupled than the protons mentioned above. This is probably due to the oscillatory behavior of TOCSY transfer, which vanishes for the chosen mixing time for the pair of geminal protons at 2.6 and 2.7 ppm. The example shows that a careful analysis of ROESY spectra is mandatory for signals close to the diagonal.

ROE rate of only $^1/_4\sigma_{ROE}$ or $^1/_2\sigma_{ROE}$ on resonance,[30] since $w_l = w_t = {}^1/_2$. It is therefore of interest to increase the weight of transverse cross relaxation. This can be achieved using shaped pulses (Figure 20.8b), or by the introduction of delays into the sequence (Figure 20.8c).

In the following, ROESY sequences will be compared that yield equal net cross-relaxation rates on-resonance and that dissipate the same power in a sample. Figure 20.9 shows the offset behavior of cross relaxation of JS ROESY [(a): $\theta = 53.77^\circ$] and of a phase-alternating ROESY employing a shaped 180° pulse to increase w_t.[31]

The offset dependence of the cross relaxation of the JS ROESY sequence is somewhat less pronounced than that of the phase-alternating sequence.

In Figure 20.9(c), the scaling λ is plotted as a function of the offset for both sequences. The minimal λ of the two spin locks is plotted for JS ROESY, since λ may not be averaged in the case of extended stretches of CW irradiation. On-resonance, λ is larger for JS ROESY than for the phase-alternating sequence. This result is a direct consequence of the fact that the scaling of λ in CW sequences is minimal at given w_t. For larger offsets, the phase-alternating sequence yields a somewhat better suppression of TOCSY (larger λ). Although λ can serve as a measure of TOCSY transfer along the diagonal only, this reasoning shows that it appears to be worthwhile to search for optimized ROESY sequences that minimize the loss in λ on-resonance while achieving maximum λ off-resonance.

Figure 20.10 shows a comparison of JS ROESY and the phase-alternating ROESY sequence. The spectra differ only marginally. Coherent transfer is well suppressed, except for the two strongly coupled geminal protons H-6′, H-6″. For more details, see the figure legend.

REFERENCES

1. L. Braunschweiler and R. R. Ernst, *J. Magn. Reson.*, 1983, **53**, 521.
2. A. A. Bothner-By, R. L. Stephens, J. M. Lee, C. D. Warren, and R. W. Jeanloz, *J. Am. Chem. Soc.*, 1984, **106**, 811.
3. T. E. Bull, *J. Magn. Reson.*, 1988, **80**, 470; T. E. Bull, in *Progress in Nuclear Magnetic Resonance Spectroscopy*, eds. J. W. Emsley, J. Feeney, and L. H.

Sutcliffe, Pergamon Press, Oxford, 1992, Vol. **24**, p. 377.

4. U. Haeberlen and J. S. Waugh, *Phys. Rev.*, 1968, **175**, 453.
5. Haeberlen, U. *High Resolution NMR in Solids*, Academic Press, New York, 1976, pp. 47.
6. R. R. Ernst, G. Bodenhausen, and A. Wokaun, *Principles of Nuclear Magnetic Resonance in One and Two Dimensions*, Oxford University Press, Oxford, 1987.
7. F. J. Dyson, *Phys. Rev.*, 1949, **75**, 486, 1736.
8. R. P. Feynman, *Phys. Rev.*, 1951, **84**, 108.
9. W. Magnus, *Commun. Pure Appl. Math.*, 1954, **7**, 649.
10. J. S. Waugh *J. Magn. Reson.*, 1986, **68**, 189.
11. S. J. Glaser and G. P. Drobny, in *Advances in Magnetic Resonance*, ed. W. S. Warren, Academic Press, New York, 1990, Vol. **14**, p. 35.
12. J. S. Waugh, *J. Magn. Reson.*, 1982, **50**, 30.
13. C. Griesinger and R. R. Ernst, *Chem. Phys. Lett.*, 1988, **152**, 239.
14. J. Schleucher, J. Quant, S. J. Glaser, and C. Griesinger, *J. Magn. Reson. A*, 1995, **112**, 144.
15. A. Bax and D. G. Davis, *J. Magn. Reson.*, 1985, **65**, 355.
16. A. J. Shaka, J. Keeler, and R. Freeman, *J. Magn. Reson.*, 1983, **53**, 313.
17. S. P. Rucker and A. J. Shaka, *Mol. Phys.*, 1989, **68**, 509.
18. M. Kadkhodaie, O. Rivas, M. Tan, A. Mohebbi, and A. J. Shaka *J. Magn. Reson.*, 1991, **91**, 437.
19. C. Griesinger, G. Otting, K. Wüthrich, and R. R. Ernst, *J. Am. Chem. Soc.*, 1988, **110**, 7870.
20. J. Cavanagh and M. Rance, *J. Magn. Reson.*, 1992, **96**, 670.
21. U. Kerssebaum, R. Markert, J. Quant, W. Bermel, S. J. Glaser, and C. Griesinger, *J. Magn. Reson.*, 1992, **99**, 184.
22. J. Briand and R. R. Ernst, *Chem. Phys. Lett.*, 1991. **185**, 276.
23. M. Kadkodaei, T.-L. Hwang, J. Tang, and A. J. Shaka, *J. Magn. Reson., Ser. A*, 1993, **105**, 104.
24. J. Quant, Diploma Thesis, University of Frankfurt, 1992.
25. M. Ravikumar and A. A. Bothner-By, *J. Am. Chem. Soc.*, 1993, **115**, 7537.
26. A. Bax and D. G. Davis, *J. Magn. Reson.*, 1985, **63**, 207.
27. C. Griesinger and R. R. Ernst, *J. Magn. Reson.*, 1987, **75**, 261.
28. D. Neuhaus and J. Keeler, *J. Magn. Reson.*, 1986, **68**, 568.
29. J. Cavanagh and J. Keeler, *J. Magn. Reson.*, 1988, **80**, 186.
30. T.-L. Hwang and A. J. Shaka, *J. Am. Chem. Soc.*, 1992, **114**, 3157.
31. T.-L. Hwang, M. Kadkhodaei, A. Mohebbi, and A. J. Shaka, *Magn. Reson. Chem.*, 1992, **30**, S24.
32. J. Fejzo, W. M. Westler, S. Macura, and J. L. Markley, *J. Magn. Reson.*, 1991, **92**, 20.